NASA Technical Memorandum 82697
AIAA-81-1965

# Acoustic Performance of Inlet Suppressors on an Engine Generating a Single Mode

L. J. Heidelberg, E. J. Rice,
and L. Homyak
*Lewis Research Center*
*Cleveland, Ohio*



...ared for the
Seventh Aeroacoustics Conference
sponsored by the American Institute of
Aeronautics and Astronautics
Palo Alto, California, October 5-7, 1981


NASA

# ACOUSTIC PERFORMANCE OF INLET SUPPRESSORS ON AN ENGINE GENERATING A SINGLE MODE

by L. J. Heidelberg, E. J. Rice and L. Homyak

National Aeronautics and Space Administration
Lewis Research Center
Cleveland, Ohio 44135

## Abstract

As part of a program to evaluate an inlet suppressor design method based on mode cutoff ratio, three single degree of freedom liners with different open area ratio face sheets were designed for a single spinning mode. This mode was generated by placing 41 rods in front of the 28 blade fan of a JT15D turbofan engine. At the liner design this near cutoff mode has a theoretical maximum attenuation of nearly 200 dB per L/D. The data show even higher attenuations at the design condition than predicted by the theory for dissipation of a single mode within the liner. This additional attenuation is large for high open area ratios and should be accounted for in the theory. The data shows the additional attenuation to be inversly proportional to acoustic resistance. It was thougnt that the additional attenuation could be caused by reflection and modal scattering at the hard to soft wall interface. A reflection model was developed, and then modified to fit the data. This model was checked against independent (multiple pure tone) data with good agreement.

E-980

## Introduction

Fan noise produced by an aircraft engine has a spinning mode structure while propagating within the inlet or aft ducts. These spinning modes must be considered in the design of an effective suppressor.[1-3] A theoretical design method based on mode cutoff ratio is presented in Ref. 4. This method and the general problem of designing and evaluating inlet suppressors from source to far-field is based upon each element of the problem being dependent upon the mode cutoff ratio. This dependence upon cutoff ratio has been reported for maximum possible attenuation,[4] optimum impedance,[5] duct termination reflection,[6] and modal density function.[7]

The above concepts were evaluated on a YF102 engine both qualitatively[8] and quantitatively[9] using the multimodal sound source due to fan turbulence interaction. These evaluations of the design methods and theories were extremely demanding and were limited by the source energy being distributed among all possible propagations modes.

In this investigation, a JT15D engine was modified to produce a fan tone controlled by a single mode that could be used to validate the design theory and theoretical suppressor performance described in Refs. 4 to 9. To the best of the authors' knowledge, this is the first time that a controlled known single mode has been used with an engine or fan to evaluate suppressors. The single mode is generated by placing 41 equally spaced rods in front of the 28 blade fan as shown in Fig. 1. These rods produce a blade

passing frequency (BPF) tone of only one mode with circumferential order $m = 13$ and the lowest radial order $\mu = 0$ at fan speeds from 6400 to 8400 rpm. The design speed for the suppressors was chosen as 8750 rpm where the cutoff ratio of the 13, 0 mode was 1.03. Tests were conducted at the design speed as well as higher speeds including a supersonic fan tip speed.

The suppressor theory, used to compare with the data, contains only the dissipation effect of the liner on the mode corresponding to the input mode in the hardwall duct. It was found necessary to account for additional attenuation due to reflection or modal scattering at the hardwall-liner interface. A model was derived to account for this effect.

## Symbols

| | |
|---|---|
| $A$ | additional attenuation above liner dissipation, dB |
| BPF | blade passage frequency, Hz |
| $c$ | speed of sound, m/sec |
| $D$ | circular duct diameter, m (ft) |
| $\Delta dB$ | sound attenuation, decibels |
| $\Delta dB_m$ | maximum possible sound power attenuation, decibels |
| $f$ | frequency, Hz |
| $K_{XH}$ | dimensionless axial wave number for spinning mode in hard wall duct (see Eq. 9) |
| $K_{XS}$ | dimensionless axial wave number for spinning mode in soft wall duct |
| $L$ | length of acoustic treatment, m (ft) |
| $M_0$ | axial steady flow Mach number, free-stream uniform value |
| $m$ | spinning mode lobe number (circumferential order) |
| $R$ | pressure reflection coefficient |
| $RR^*$ | reflected acoustic power, dB |
| $R_g$ | eigenvalue for circular hardwalled duct or absolute value of complex eigenvalue for softwall duct |
| $\eta$ | frequency parameter, $\eta = fD/c$ |
| $\theta$ | specific acoustic resistance |
| $\theta_m$ | optimum specific acoustic resistance |
| $\mu$ | radial mode order index |
| $\xi_H$ | hardwall cutoff ratio, $\xi_H = \dfrac{\pi\eta}{R_g\sqrt{(1 - M_0^2)}}$ |
| $\xi_S$ | softwall mode cutoff ratio, $\xi_S = \dfrac{\pi\eta}{R_g\sqrt{(1 - M_0^2)\cos 2\phi}}$ |
| $\sigma$ | liner open area ratio |
| $\sigma_m$ | optimum open area ratio |
| $\phi$ | phase of complex eigenvalue, degrees |
| $X$ | specific acoustic reactance |

## Apparatus and Procedure

### Engine and Inlet

The JT15D-1 engine is a two-spool turbofan engine with a nominal 3.3 bypass ratio, and a rated thrust of 9790 N (2200 lb). The fan is 53.3 cm (21 in.) in diameter, and has 28 blades with 66 exit guide vanes (stator). The blade to vane number ratio for this fan results in a cutoff rotor-stator interaction tone. More details for this engine are presented in Ref. 10.

The inlet used in this investigation is shown in Fig. 1. This inlet has a constant 53.3 cm (21 in.) diameter and is fitted to a bellmouth which in turn is attached to a large constant diameter nacelle. A large inflow control device (ICD) constructed of aluminum honeycomb, screen and thin steel ribs is attached to the nacelle. The ICD removes large scale atmospheric turbulence and thus greatly reduces the BPF tone that results from the interactions of the fan with this turbulence.[10] The ICD was used here to further insure that only a single mode BPF tone is produced.

A spool piece with 41 equally spaced radial rods was attached to the engine front flange. The wakes of these rods interact with the 28 fan blades to produce a BPF tone with 13 circumferential lobes. At fan speeds between 6400 and 8400 rpm only the lowest radial order mode can propagate. A more complete description of the fan-rod interaction tone is presented in Ref. 11.

The single degree of freedom, SDOF type acoustic treatment was placed just up stream of the rod section of the inlet. This suppressor section is replaceable so that different treatment designs can be tested.

### Suppressor Design

The acoustic liners were designed to heavily attenuate the single mode produced by the interation of the inlet rods and the engine fan. This mode is the lowest radial of the thirteen lobed circumferential pattern ($m = 13$, $\mu = 0$). Maximum attenuation was sought for this mode at the blade passage frequency of 3150 Hz. Other parameters pertinent to the design were average duct Mach number ($M_D$) of -0.147, duct diameter of 53.3 cm (21 in.), and boundary layer thickness (1/7th power) of 0.53 cm (0.21 in.) based upon an estimate made from velocity measurements.

The optimum impedance was calculated using the sound propagation theory of Ref. 12 and the optimization procedure of Ref. 13. The theory considers the propagation of spinning modes in an acoustically treated semi-infinite cylindrical duct with a steady flow. The flow is assumed uniform except near the wall where a 1/7th power boundary layer (with a linear profile at the wall) is merged with the uniform flow.

The impedance model used to define the suppressor construction (perforated plate bonded to honeycomb) can be found in Ref. 8. The acoustic resistance model is a slight modification of the model of Ref. 14, and assumes that steady grazing flow effects dominate the perforated plate acoustic resistance (sound amplitude effect neglected).

The results of the liner optimization calculations can be found in Table I. The values in the middle column, with a perforated plate open area ratio of 5 percent, describe the estimated optimum liner. It should be noted that no accounting of the inevitable perforated plate hole blockage (when

bonded to honeycomb) was made. Also because of uncertainties in the acoustic resistance model and the measured design inputs (flow Mach number, boundary layer thickness), it was determined that liners at one-half and double the optimum liner resistance would be built. It was also desired that the experimental liners straddle the best possible liner so that interpolations could be made using the data and the theory. Thus two liners with open areas of 2.5 and 8.9 percent were built. Note that the optimum reactance (which is obtained with more confidence) was held constant in all cases by varying the depth of the treatment.

The theoretical calculations for the optimum liner showed that the maximum possible attenuation (due to dissipation only in the liner) was $\Delta dB_m = -198$ dB per unit L/D. This extremely large expected attenuation suggested that the very short liners shown (L = 6.3 in., 16 cm) must be used to obtain meaningful measurements of attenuation. As will be seen in a later section, due to the unprecedented attenuations attained, half of this length had to be covered with tape so that the fan tone data would not be lost in the broadband noise floor.

## Test Facility

The tests were performed at the Lewis Vertical Lift Facility. This facility is an outdoor test stand sheltered by a service building which was moved away on tracks before testing. The area beneath the engine out to and somewhat beyond the far-field microphones was paved with concrete. The engine was mounted 2.9 m (9.5 ft) or 5.4 fan diameters above the ground. This relatively high position was chosen to minimize ground plane effects on the inlet flow. The engine exhaust was connected to a large muffler to suppress aft fan and jet noise. A photograph of the engine on the test stand is shown in Fig. 2.

## Acoustic Instrumentation and Processing

Far-field noise measurements were made with microphones on a 24.4 m (80 ft) radius arc centered on the engine inlet. The microphones were positioned at 10° intervals from 10° to 120° from the inlet axis. The 1.25 cm (0.5 in.) diameter microphones were mounted on 61 cm (2 ft) square composition hard boards at ground level and pointed at the engine inlet.

The microphone signals were recorded on magnetic tape and then processed on a spectrum analyzer. The one-third-octave-band results were corrected to a 30.5 m (100 ft) free-field radial distance and standard-day temperature and relative humidity (59° F and 70 percent, respectively). The correction applied to the ground microphone data to obtain free-field levels was -6.0 dB at all frequencies up to 20 kHz.

The narrow band data were processed on a separate 800 line spectrum analyzer. Narrow band results were not corrected but used and presented in the "as measured" form.

## Test Procedure

For all tests, data were obtained at the following corrected fan speeds: 6750, 8450, 10 500 and 13 500 rpm. At the experiment design

speed of 6750 rpm a second set of data was measured to improve accuracy. A baseline hard wall case was always run the same day to improve the quality of the attenuation results. The hardwall case was obtained by covering the acoustic liner with aluminum tape. After the baseline was obtained, the tape was removed in two stages to obtain measurements for treatment lengths of L/D of 0.15 and 0.3. Data was only recorded when the ambient wind was less than 18.5 km/hr (10 mph).

## Results and Discussion

The data is presented in both one-third-octave-band and narrow band form. A 25-Hz bandwidth narrowband analysis was used where the broadband noise floor affects the accuracy of the one-third-octave-band tone data. All one-third-octave-band data has been corrected to standard-day, free-field at 30.5 m (100 ft). Narrow-band data has not been corrected, and is presented "as measured".

### Baseline Inlet Noise

The inlet noise of the unsuppressed engine with the 41 rods installed is shown by the four one-third-octave power spectra in Fig. 3. The BPF is very prominent at all four speeds. At the highest speed (tip relative Mach number of 1.2), the multiple pure tones, MPT's are very evident between 2000 and 4000 Hz. The dashed line represents the power spectra for a suppressed case, the 8.9 percent open area liner with an L/D of 0.15. This gives an indication of where the liner was effective. At design speed the BPF tone is no longer evident in the spectrum. The only other place where there is a great deal of suppression is at 13 500 rpm at the MPT frequencies. The reason for this behavior will be discussed later after tone directivities and cutoff ratios are presented. Although the suppressions at the other speeds and frequencies are much lower, they are not insignificant, 10 to 20 dB per unit L/D.

The one-third-octave BPF tone directivities for all the fan speeds are shown in Fig. 4. At a fan speed of 6750 rpm the (13,0) mode is just cut on with a cutoff ratio of 1.03. All higher order radial modes are cutoff. The peak in the directivity plot is at 60° as would be expected for a mode near cutoff.[11] As the fan speed increases the cutoff ratio of the (13,0) mode increases and the directivity curve peaks at far field angles closer to the inlet axis. This effect can be masked (as in Fig. 4(d)) when higher order radial modes being propagating (10 500 rpm and above) and the directivity pattern is a result of several modes of different cutoff ratio. A more complete discussion of the BPF directivity of this fan with the 41 rods is presented in Ref. 11.

These directivity patterns are important since they can indicate the modes and corresponding cutoff ratios that are present.[6] The cutoff ratio in turn controls the maximum possible attenuation and optimum impedance for a suppressor.[4]

## Suppressor Performance

The sound power attenuation curves shown in Fig. 5 give an overview of where attenuation was obtained in terms of frequency and speed. The curves shown are for the 8.9 percent liner with an L/D of 0.15. This was the most effective liner. The other liners yielded similar curves but with lower peak levels. Except at the design speed the BPF attenuation is of the order of 2 to 3.7 dB, or on a unit L/D basis, 13 to 25 dB. At the design speed 12.5 dB of BPF power reduction was obtained, or 83 dB per unit L/D. This number is in error on the low side due to the dominant contribution of the broadband noise to the BPF one-third-octave-band at many angles in the suppressed case.

The liners were designed for the (13,0) mode at 3150 Hz where the cutoff ratio is 1.03. In general, it would be expected that when the cutoff ratio is higher or the frequency different than the design, lower attenuation would result. The maximum possible attenuation decreases very rapidly when the cutoff ratio increases from unity.[4] Also the optimum impedance for a given mode is a function of cutoff ratio and frequency.[5] For these reasons the large BPF attenuation occurs only at the design speed and since the cutoff ratio increases with speed and the actual wall impedance diverges from the optimum, the attenuation drops. This dramatic change in liner attenuation with engine speed does not occur for multimodal excitation as was observed in Ref. 8. An examination of the source noise in this investigation shows only two places where single modes exist near cutoff. One is the design condition and the other is the MPT's at supersonic blade tip speeds. The MPT cutoff ratios vary from 1.00 to 1.07. Figure 5(d) shows a great deal of attenuation for these MPT's as is expected. In fact, the MPT that corresponds to the design frequency, 3150 Hz has a cutoff ratio of 1.03, the same as the BPF had at the design point. The MPT results will be discussed in more detail later in this paper.

## BPF at the Design Point

A typical one-third-octave-band directivity plot of the BPF is shown in Fig. 6. Here the short liner length (L/D = 0.15) produced a large reduction in tone level especially at the peak angle (60°) and larger angles. When the remaining half of the tape was removed (L/D = 0.3) little further reductions occurred due to the presence of the broadband noise floor. Even in a 25 Hz bandwidth analysis the broadband floor interferes with the results for an L/D of 0.3. The narrowband results for this liner (Fig. 7) indicate tone level reductions of several dB more than shown by the one-third-octave plot for the L/D of 0.15. Here the narrowband (25 Hz bandwidth) tone directivity is plotted for the hardwall inlet and for the 8.9 percent open area liner at the L/D of 0.15. The broadband noise level at the tone base is also plotted. Even with an L/D of only 0.15 and a 25 Hz bandwidth, the broadband levels are uncomfortably close to the tone in the suppressed case. Although the broadband levels show a small reduction in level when compared to the tone these attenuations are significant when put on a unit L/D basis, 15 to 20 dB. The shape of the broadband directivity curve, with a peak near the axis, indicates this source is composed of a great many modes with approximately equal energy per mode.[6] With this

type of modal energy distribution much lower attenuations are expected than when all the energy is concentrated in one near cutoff mode.

The directivity of the tone suppression at the design condition for all three liners is shown in Fig. 8. The suppression generally increase to about 60 degrees then remains at high levels. The 2.5 percent open area liner has about half the suppression of the other two liners. The 8.9 percent liner appears to give somewhat better suppression than the 5.0 percent liner.

One way to show the effect of open area ratio on attenuation is to use the following approximate relationship from Ref. 15:

$$\Delta dB \propto \frac{\Theta_m}{\Theta} \tag{1}$$

when

$$\Theta > \Theta_m$$

and

$$\Delta dB \propto \frac{\Theta}{\Theta_m} \tag{2}$$

when

$$\Theta < \Theta_m$$

This approximation can be put in terms of liner open area ratio by using

$$\Theta \propto \frac{(1 - \sigma^2)}{\sigma} \tag{3}$$

This results in

$$\Delta dB \propto \frac{(1 - \sigma_m^2)\sigma}{(1 - \sigma^2)\sigma_m} \tag{4}$$

when

$$\sigma < \sigma_m$$

and

$$\Delta dB \propto \frac{(1 - \sigma^2)\sigma_m}{(1 - \sigma_m^2)\sigma} \tag{5}$$

/

when

$$\sigma > \sigma_m$$

In Fig. 9 attenuation is plotted against the above open area ratio functions. It was assumed that the optimum area is between 5.0 and 8.9 percent i.e., straight lines from the origins through the 5.0 and 8.9 percent points meet at the optimum open area ratio. The average attenuation between 50° and 80° was used as an indication of sound power attenuation of the BPF tone at the design speed. Although the 2.5 percent data was not used in the data fit, it falls on the line. Fitting the data through the 5.0 and 8.9 percent points as described above results in an optimum open area ratio of 7.1 percent. This is higher than the design estimate of 5.0 percent but not that far away when consideration is given to the assumptions and variables involved. For example, an error in the boundary layer thickness used to calculate the resistance could account for all of the difference between the 5.0 and 7.1 percent. Also, the reduction of open area due to the adhesive used to bond the face sheet was not accounted for. The theoretical attenuation limit for the (13,0) mode is included in Fig. 9. The data plot indicates a peak of 27.2 or 181 dB per unit L/D. This is very good agreement with the theoretical limit of 198 dB per unit L/D.

Off-optimum liner attenuation. - As discussed in the liner design section it was not anticipated that the optimum liner design would truly be achieved and two extra liners were built. It is thus necessary to investigate how much acoustic dissipation might be expected within the suppressor for conditions other than at the optimum. Also in spite of the large attenuations expected, it will be seen later that even higher attenuations were obtained from the suppressor experiments. A complete set of theoretical predictions of single mode acoustic dissipation in the liner is necessary for comparison with the experimental data.

To evaluate off-optimum sound attenuations in the suppressor, the approximate circular constant attenuation contour equation found in the appendix of Ref. 9 was used. This correlation provides good approximation to exact suppressor calculations. The inputs used for this equation involve only the optimum impedance and the associated maximum possible attenuation which were $\Theta_m = 1.1360$, $X_m = -0.50$, $\Delta dB_m/L/D = 198$ respectively, the duct Mach number $M_D = -0.147$, and the soft-wall mode cutoff ratio $\xi_s = 0.8291$. Due to the small cutoff ratio the compression of the attenuation contours due to the boundary layer can be neglected. For all calculations the liner reactance was assumed to be equal to the optimum value.

With the above inputs, the liner resistance can be varied from zero to infinity to generate the relationship shown in Fig. 10. The curve has the extremely sharp peak which is characteristic of the attenuation for a single mode as generated for tests in this paper. For multimodal sound generation much more flat curves will result as discussed in Ref. 9. Note that the attenuation shown in Fig. 10 accounts only for principal mode dissipation within the lined duct. Any attenuation greater than these values may be assumed to originate from other mechanisms such as reflection or modal scattering at the hard-soft interface of the suppressor. This assumption will be used to develop relations for these other phenomena in a later section.

The data is plotted in Fig. 10 for two different optimum resistances (open areas). In one case the 2.5 percent point is made to fall on the theoretical curve, which results in an optimum open area of 5.4 percent, and in the other case the optimum was chosen at 7.0 percent. In general, the data falls above the curve for most $\sigma_m$ that are chosen. It seems likely, as discussed previously, that reflections and modal scattering from the hard to soft wall interface could cause the data to fall above the curve. It might be expected the larger the change in wall resistance at the interface the larger the reflection and modal scattering. Since the 2.5 percent open area liner might be expected to have little or no reflection it was made to fall on the theoretical attenuation curve. This resulted in the 5.0 percent liner data falling below the curve. It seems reasonable that the data could be higher than theory expecially for the liners with higher open area ratios. It is more difficult to understand why a data point would fall below the curve as in the case of the 5.0 percent liner, when the other points are on or above. The data points seem to fall in a more reasonable fashion when the optimum open area is chosen at 7.0 percent. Here the points fall progressively higher above the curve as the open area increases. If additional attenuation caused by the hard to soft wall interface is the major cause of the discrepancy, it is important because of its size to account for it in the theory. The largest discrepancy occurs in the 8.9 percent data where 36 percent of the total attenuation may be due to mechanisms other than dissipation within the lined duct.

If the strength of the additional attenuation above liner dissipation is plotted against the reciprocal of open area ratio (resistance) on log-log scale, a functional relation of the variables may become evident. This plot was made for a range of $\sigma_m$ and a straight line resulted when $\sigma_m = 7.0$ percent as shown in Fig. 11. The slope of this line turns out to be -1.0. This plot not only indicates that 7.0 percent open area is optimum, but also that at a fixed cutoff ratio and liner reactance, the additional attenuation due to the hard to soft wall interface is inversely proportional to resistance.

Reflection and scattering. - The previously discussed comparison between theory and experiment for the suppression of the blade passage tone has shown that more attenuation is attained than can be explained by simple dissipation of the principal mode within the suppressor. This suggests that additional attenuation mechanisms are operating which are not included in the suppressor theory. These many include reflection and scattering at the hard-soft interface of the suppressor. An approximate equation for the reflection effect will be derived (scattering will be neglected) to provide a hint on the grouping of the important variables and then the equation will be empirically modified to fit the blade passage frequency attenuation data. Without further modification this equation will be used to calculate the additional attenuation of several multiple pure tones and the results will be compared to data in the next section.

Reflection and scattering are intimately connected but reflection is qualitatively different than dissipation. No dissipation can be expected for nearly hard walls ($\theta \approx \omega$) or for very soft walls ($\theta \approx 0$) since hard walls allow no normal flow into them and very soft walls have no acoustic resistance to provide dissipation. Since the two extremes provide no dissipation peak dissipation must occur somewhere between and this is the optimum impedance which was discussed earlier. Reflection, although expected to be zero for

hardwalls, is not necessarily negligible for soft walls. There may be a monotonic increase in reflection as resistance is reduced, and the overall optimum resistance might be expected to be slightly shifted toward a smaller resistance than would be obtained from a dissipation only theory.

In Ref. 16 (page 1528) the reflection coefficient for a plane-wave incident upon a suppressor has been derived. It is desired here to obtain an expression for incident spinning modes rather than for the special case of a plane wave with an infinite cutoff ratio. A mode matching solution with pressure and axial velocity matching across the hard-soft interface (considering only a single spinning mode) provides a lead term in the solution which is analagous to that of Eq. 11.4.26 of Ref. 16. This equation is

$$R = \frac{k_{XH} - k_{XS}}{k_{XH} + k_{XS}} \tag{6}$$

where $R$ is the pressure reflection coefficient, and $k_{XH}$ and $k_{XS}$ are the dimensionless axial wave numbers for the spinning mode in the hard and soft duct sections. Equation (6) is accurate in the limit for nearly hard walls. The finite mode cutoff ratio, $\xi$ is present in the axial wave number. An inspection of Eq. 11.4.26 of Ref. 16 shows indexed multiple products which represent the scattering effect of higher radial modes which is neglected here.

An expansion of Eq. (6) around nearly hard walls with the parameter

$$\varepsilon = \frac{i\pi n}{\theta + iX} = \frac{\pi n(X + i\theta)}{(\theta^2 + X^2)} \tag{7}$$

considered small yields

$$R = \frac{1}{1 - 2\pi n\, k_{XH}^2 (X + i\theta)} \tag{8}$$

where

$$k_{XH}^2 = 1 - \frac{1}{\xi_H^2} \tag{9}$$

and $\xi_H$ is the mode cutoff ratio in the hard duct. An estimate of the reflected acoustic power is

$$RR^* = \frac{1}{\left(1 + 2\pi n\, k_{XH}^2 X\right)^2 + \left(2\pi n\, k_{XH}^2 \theta\right)^2} \tag{10}$$

and the attenuation due to reflection is

$$\Delta dB_R = 10 \log (1 - RR^*) \tag{11}$$

Recall that in the derivation of Eqs. (8) and (10) all scattering effects were neglected and that the results should be expected to be valid for nearly hardwalls. Considerable liberties will now be taken in the altering of these equations to match the experimental data for the blade passage frequency. It was a fortunate coincidence that for the previous blade passage tone conditions, the first term in the denominator of Eq. (10) was negligible and thus only the resistance term remained. An excellent fit to the data, as shown in Fig. 11, was obtained by changing the second power on the resistance term to the first power. Since the reactance term was negligible no information could be obtained on the exponent of this term so it was arbitrarily reduced to the first power in analogy with the resistance. The empirical final results which must be considered speculative and needing much more study are

$$RR^* = \frac{1}{\left|1 + 2\pi n K_{XH}^2 X\right| + 2\pi n K_{XH}^2 \Theta} \tag{12}$$

It was also required that Eq. (11) be changed to

$$\Delta dB_R = 40.6 \log (1 - RR^*) \tag{13}$$

to match the level of the additional attenuation that was obtained in the experiments.

Although the approach taken in this section is quite crude, perspective should be maintained by recognizing that the correlation developed relates only to the incremental attenuation shown in Fig. 10. Most of the attenuation is accounted for by the more soundly based liner dissipation theory. Equations (12) and (13) will be tested against other independent data in the next section.

MPT's at 13 500 rpm

The attenuation of the MPT's for each of the three test liners is shown as a function of hardwall cutoff ratio in Fig. 12. These attenuations are obtained using narrowband data at 60° and 70°. Some of the MPT attenuations are very large and comparable to the BPF attenuations at the design speed. This is not unexpected since each MPT is a single mode and has a cutoff ratio near unity. In general, the attenuation increases as the open area ratio increases and decreases as the cutoff ratio increases. Two sets of theoretical predictions of the attenuation for each open area ratio have been included in Fig. 12. The lower curve represents only the dissipation in the liner. The values used here for the acoustic resistance were calculated by setting the effective open area ratio to 5/7 of the actual. This reduction is based on the results for the single mode BPF data where $\sigma_m$ was shown to be 7.0 percent instead of the predicted 5.0 percent (Figs. 10 and 11). The upper curve in each set

represents liner dissipation plus the additional attenuation due to reflection and modal scattering as developed in the previous section of this paper and modified to fit the BPF data (Eqs. (12) and (13)). These upper curves fit the data well although there is considerable scatter for individual MPI's. The theoretical predictions seem valid considering they are based on independent data. The largest discrepancy occurs as the cutoff ratio approaches unity. Theoretical attenuation predictions which include mode reflection and scattering and finite liner length should be compared to this experimental data.

## Concluding Remarks

As part of a program to evaluate an inlet suppressor design method based on mode cutoff ratio, three liners with different open area ratio face sheets were designed for a single mode. This mode was generated by placing 41 rods in front of the 28 blade fan. An inflow control device was used to eliminate rotor-turbulence interaction tones. At the liner design speed and BPF this mode ($m = 13$, $\mu = 0$) is near cutoff. The theoretical attenuation limit for this condition is almost 200 dB per unit L/D. Data were also taken at higher speeds including a supersonic tip speed where MPI's were generated.

Extremely high attenuations (143 dB per unit L/D) measured were at the liner design condition. Much lower but still significant attenuations were measured at other speeds and frequencies with one exception. This was at the supersonic tip speed where the MPI's had attenuations almost as large as the BPF attenuation at the design speed. When compared to the theoretical resistance versus attenuation curve, the data at the design condition has higher attenuations. This suggests attenuation mechanisms in addition to dissipation in the lined wall. Reflection and possibly modal scattering at the hard to soft wall interface was thought to be responsible for the additional attenuation. The data indicated the additional attenuation was inversely proportional to resistance. In addition, the optimum open area ratio for liner dissipation was found to be 7.0 percent instead of the predicted 5.0 percent. Error in the boundary layer thickness and not accounting for the blockage due to the adhesive used in construction may be responsible for the difference in optimum open area. A model for reflection at the hard-soft interface was developed that indicated reflected power to be inversely proportional to the square of the acoustic resistance and reactance. The theoretical model was modified to agree with the first power relationship of resistance found in the data. The model was then tested against other independent data (MPI's) and found to be in good agreement. This preliminary reflection model requires further study. For high open area ratios and near cutoff modes the reflection at the hard to soft wall interface is a significant factor in the total attenuation.

## References


1. Yurkovich, R., "Attenuation of Acoustic Modes in Circular and Annular Ducts in the Presence of Uniform Flow," AIAA Paper 74-552, June 1974.
2. Rice, Edward J., "Spinning Mode Sound Propagation in Ducts with Acoustic Treatment," NASA TN D-7913, May 1975.

3. Motsinger, R. E., Kraft, R. E., and Zwick, J. W., "Design of Optimum Acoustic Treatment for Rectangular Ducts with Flow," ASME Paper 76 GT-113, Mar. 1976.
4. Rice, E. J., "Inlet Noise Suppressor Design Method Based Upon the Distribution of Acoustic Power with Mode Cutoff Ratio," Advances in Engineering Science, Vol. 3, NASA CP-2001, 1976, pp. 883-894.
5. Rice, E. J., "Optimum Wall Impedance for Spinning Modes - A Correlation with Mode Cutoff Ratio," Journal of Aircraft, Vol. 16, No. 5, May 1979, pp. 336-343.
6. Rice, E. J., "Multimodal Far-Field Acoustic Radiation Pattern Using Mode Cutoff Ratio," AIAA Journal, Vol. 16, No. 9, Sept. 1978, pp. 906-911.
7. Rice, E. J., "Modal Density Function and Number of Propagating Modes in Ducts," NASA TM X-73539, 1976.
8. Heidelberg, L. J., Rice, E. J., and Homyak, L., "Experimental Evaluation of a Spinning Mode Acoustic Treatment Design Concept for Aircraft Inlets," NASA TP-1613, 1980.
9. Rice, E. J. and Heidelberg, L. J., "Comparison of Inlet Suppressor Data with Approximate Theory Based on Cutoff Ratio," AIAA Paper 80-0100, 1980.
10. McArdle, J. G., Jones, W. L., Heidelberg, L. J., and Homyak, L., "Comparison of Several Inflow Control Devices for Flight Simulation of Fan Tone Noise. Using a JT15D-1 Engine," AIAA Paper 80-1025, June 1980.
11. Heidmann, M. F., Saule, A. V., and McArdle, J. G., "Predicted and Observed Modal Radiation Patterns from JT15D Engine with Inlet Rods." Journal of Aircraft, Vol. 17, No. 7, p. 493, July 1980. (Also NASA TM-79074.)
12. Rice, E. J., "Spinning Mode Sound Propagation in Ducts with Acoustic Treatment and Sheared Flow," Aeroacoustics: Fan Noise and Control; Duct Acoustics; Rotor Noise, edited by I. R. Schwartz, H. T. Nagamasu, and W. C. Strahle, AIAA Progress in Astronautics and Aeronautics, Vol. 44, American Institute of Aeronautical and Astronautics, New York, 1976, pp. 475-505. Also AIAA Paper 75-519, Mar. 1975 and NASA TM X-71672, 1975.
13. Rice, E. J., "Acoustic Liner Optimum Impedance for Spinning Modes with Mode Cutoff Ratio as the Design Criterion," AIAA Paper 76-516, July 1976; also NASA TM X-73411, 1976.
14. Hersch, A. S. and Walker, B., "Effect of Grazing Flow on the Acoustic Impedance of Helmholtz Resonators Consisting of Single and Clustered Orifices," NASA CR-3177, 1979.
15. Rice, E. J., "Attenuation of Sound in Ducts with Acoustic Treatment - A Generalized Approximate Equation," NASA TM X-71830, 1975.
16. Morse, P. M. and Feshbach, H., Methods of Theoretical Physics, Part II, McGraw-Hill, New York, 1953.

TABLE 1. - SUPPRESSOR DESIGNS FOR

THE m = 13, μ = 0 MODE

[Conditions: design frequency = 3150 Hz; duct Mach Number = -0.147; duct diameter = 21 in. (53.3 cm); optimum impedance: θ = 1.136, X = -0.50.]

| | | | |
|---|---|---|---|
| Open area,[a] σ, percent | 2.5 | 5.0 | 8.9 |
| Treatment depth, in. | 0.364 | 0.500 | 0.610 |
| Estimated resistance, θ | 2.272 | 1.136 | 0.638 |
| Estimated reactance, X | -0.50 | -0.50 | -0.50 |
| Length, L, in. | 6.3 | 6.3 | 6.3 |

[a]All facing sheets were 0.020 in. (0.051 cm) thick, perforated 3003H14 aluminum with punched holes of 0.050 in. (0.127 cm) diameter.

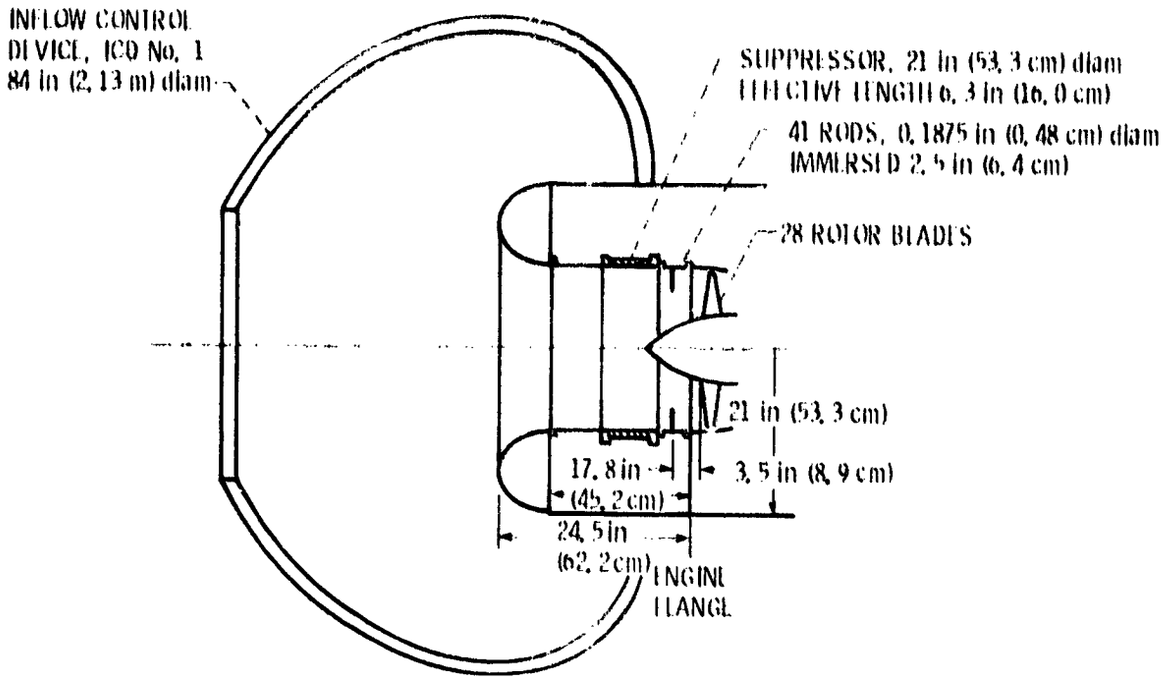


Figure 1. - Test configuration of inlet of J115D engine used for single mode SDOI suppressors.

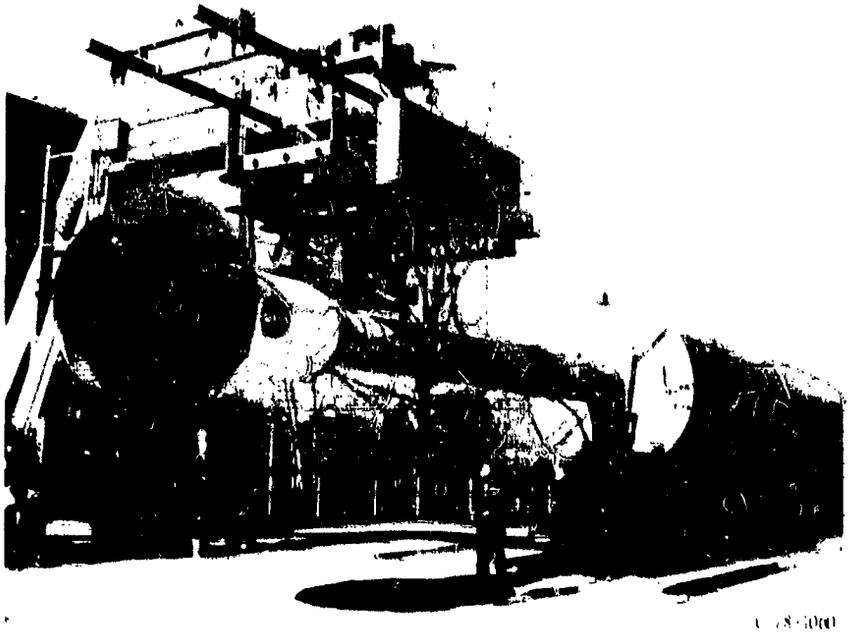

Figure 2. - J115D engine with ICD no. 1 on test stand with exhaust muffler.

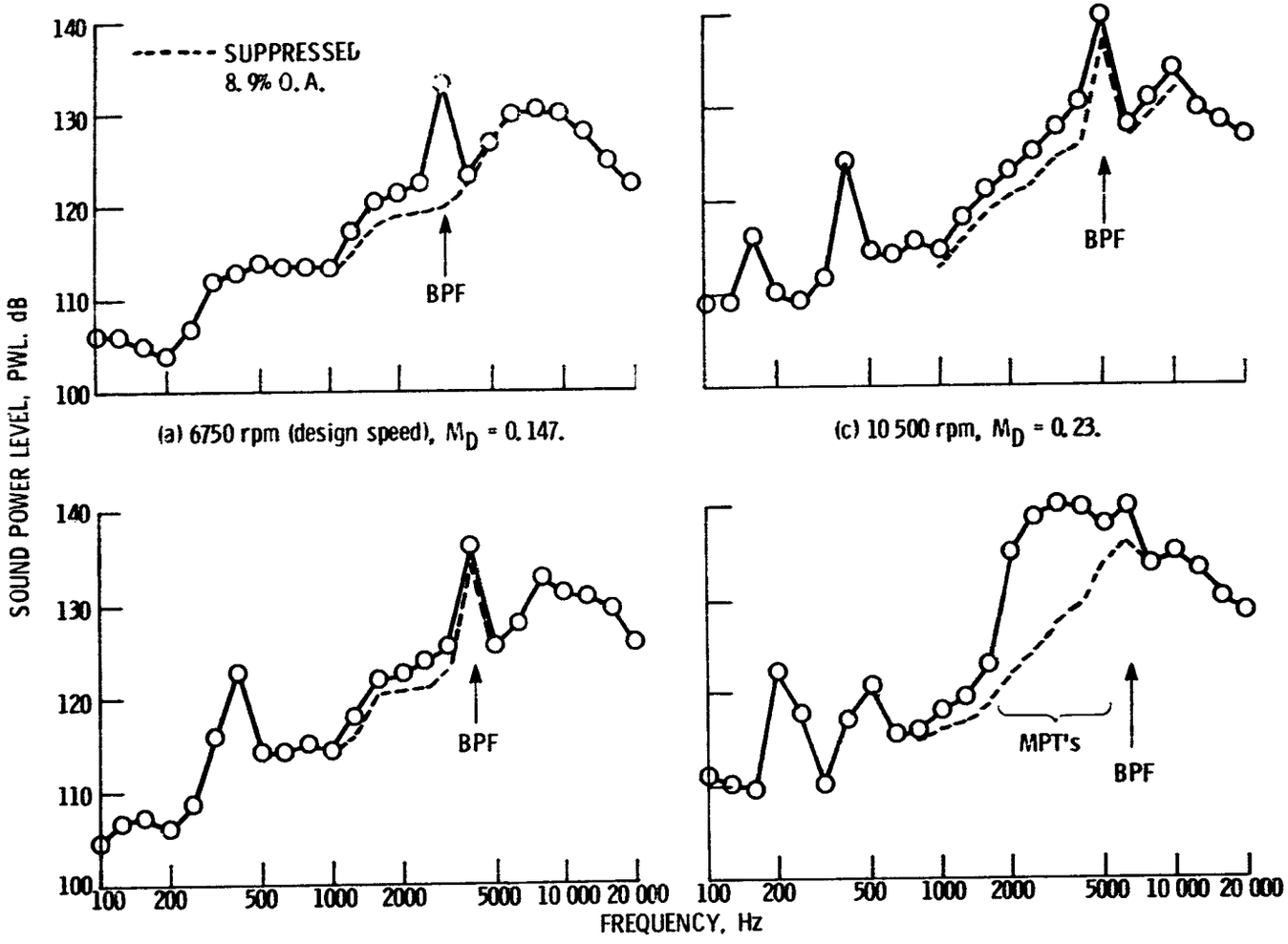


(a) 6750 rpm (design speed), $M_D$ = 0.147.

(c) 10 500 rpm, $M_D$ = 0.23.

(b) 8450 rpm, $M_D$ = 0.187.

(d) 13 500 rpm, $M_D$ = 0.33

Figure 3. - Baseline one-third-octave power spectra for 41 rod inlet configuration.

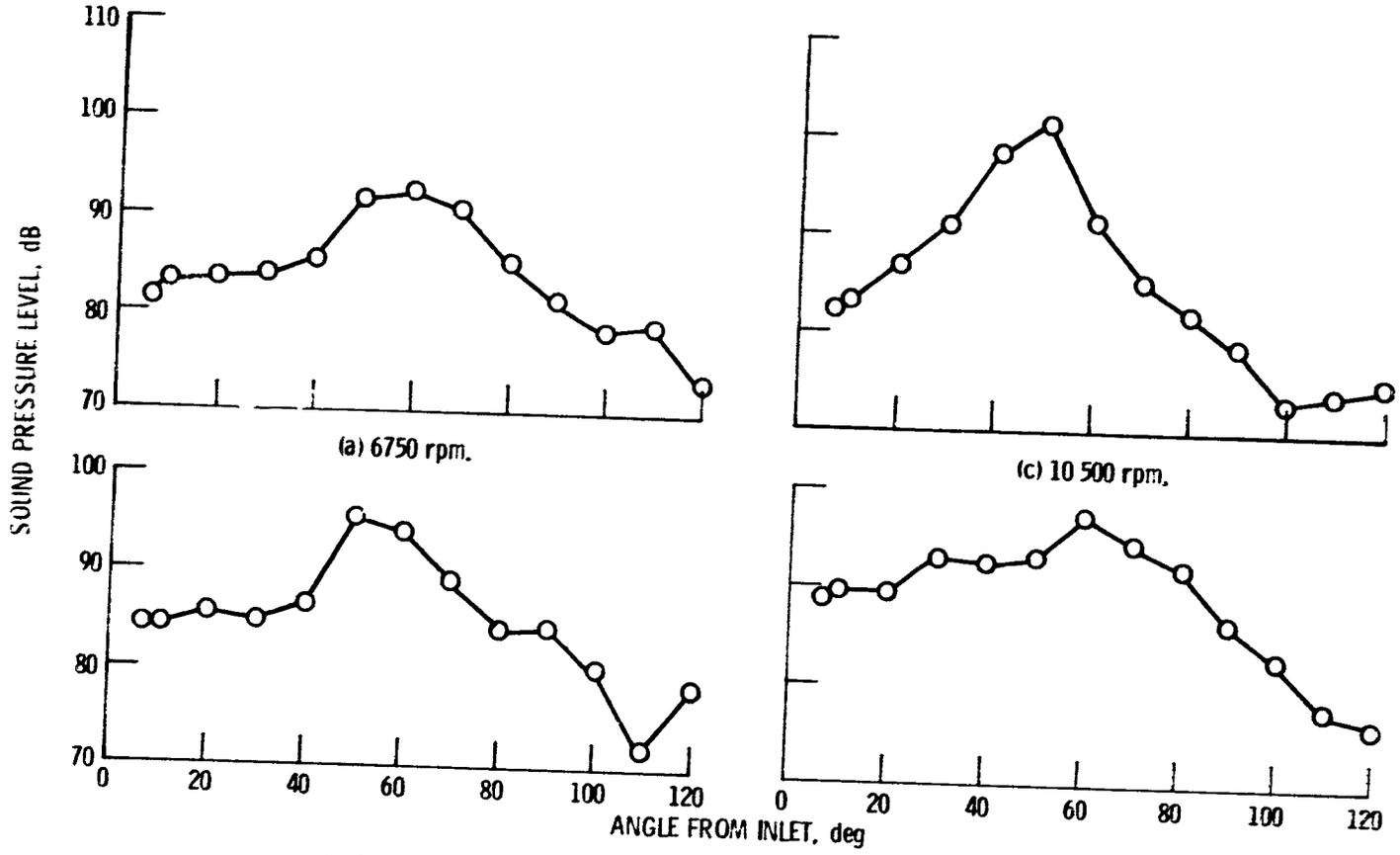


Figure 4. - One-third-octave BPF tone directivity patterns for the hardwall 41 rod baseline.

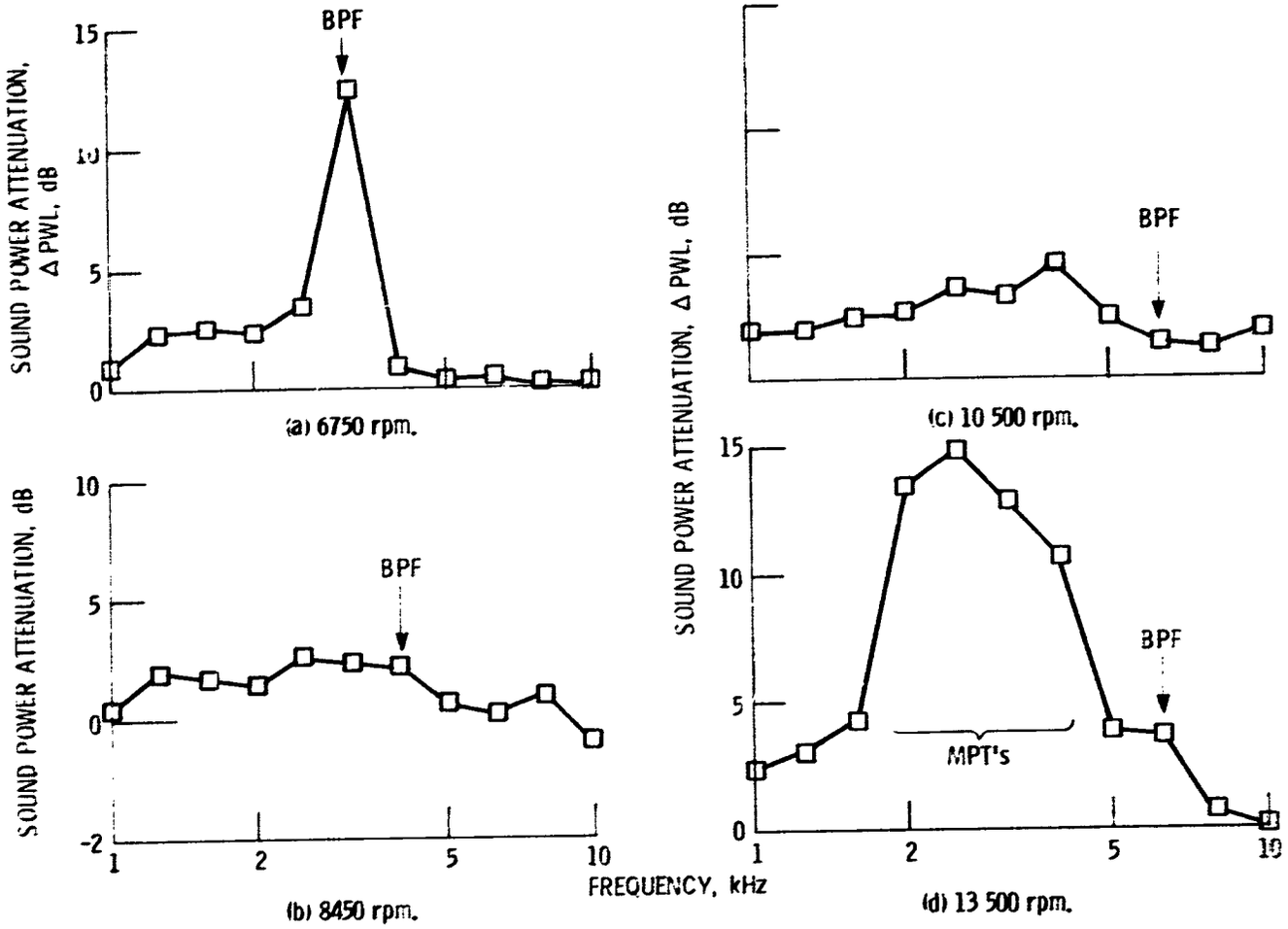


Figure 5. - One-third-octave sound power attenuation spectra for the 8.9% O.A. liner at various speeds, L/D = 0.15.

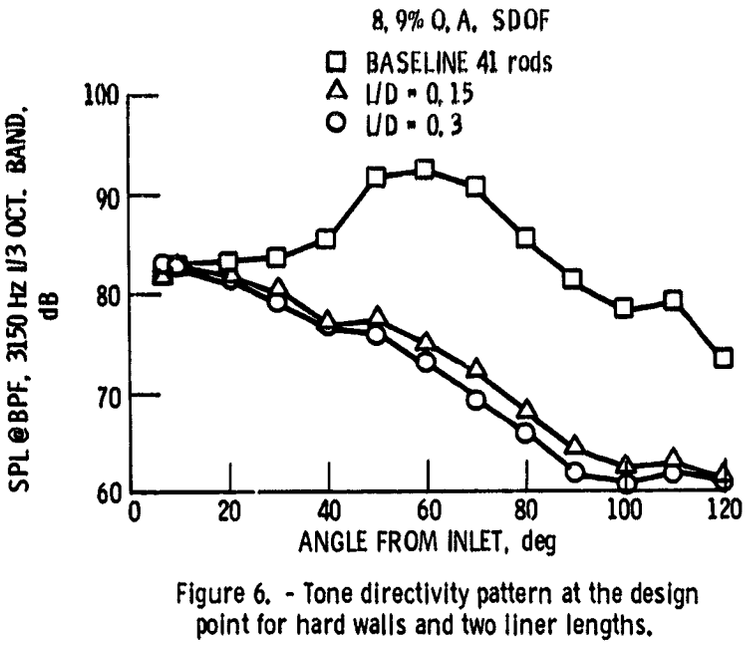


Figure 6. - Tone directivity pattern at the design point for hard walls and two liner lengths.

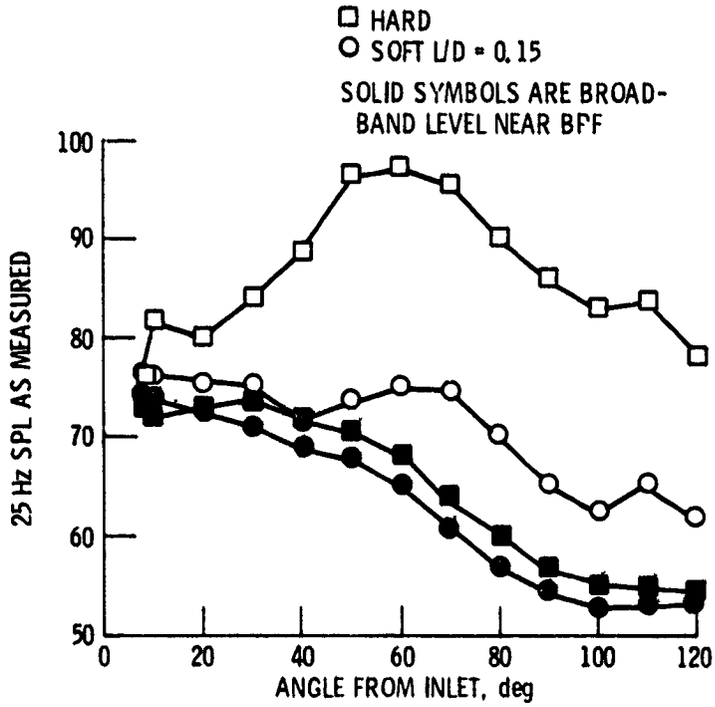


Figure 7. - Narrow band tone directivity pattern at the design point, BPF = 3150 Hz and 6750 rpm for 8.9 percent open area liner.

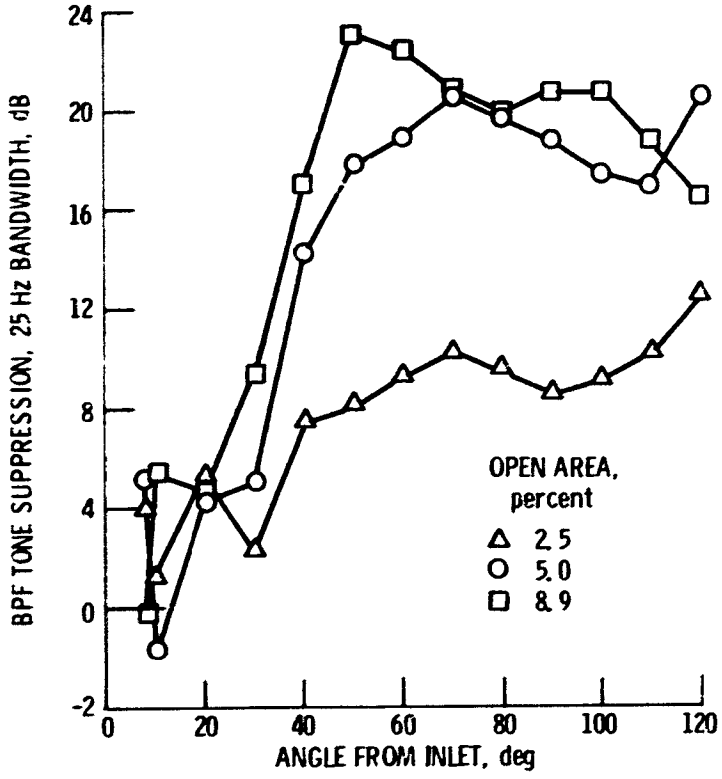


Figure 8. - Directivity of the tone suppression at the design point, BPF = 3150 Hz, L/D = 0.15.

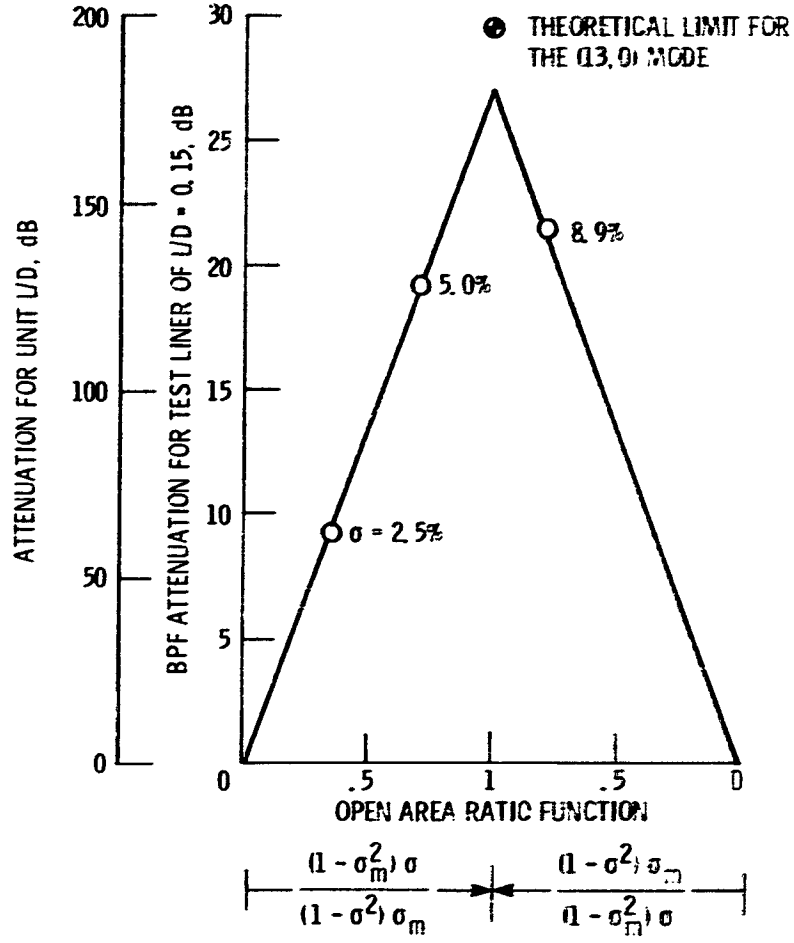


Figure 9. - Tone attenuation as a function of open area ratio, BPF = 3150 Hz, L/D = 0.15, average attenuation between 50 to 80 degrees.

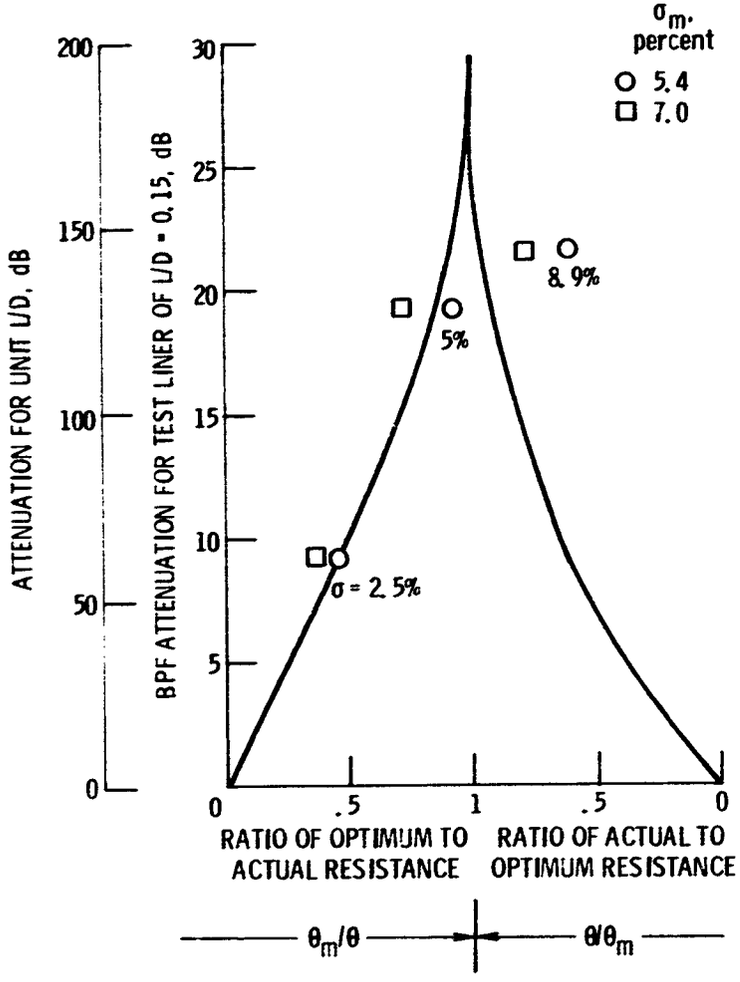


Figure 10. - Comparison of data with theoretical attenuation as a function of resistance for the (13, 0) mode at 3150 Hz and optimum reactance.

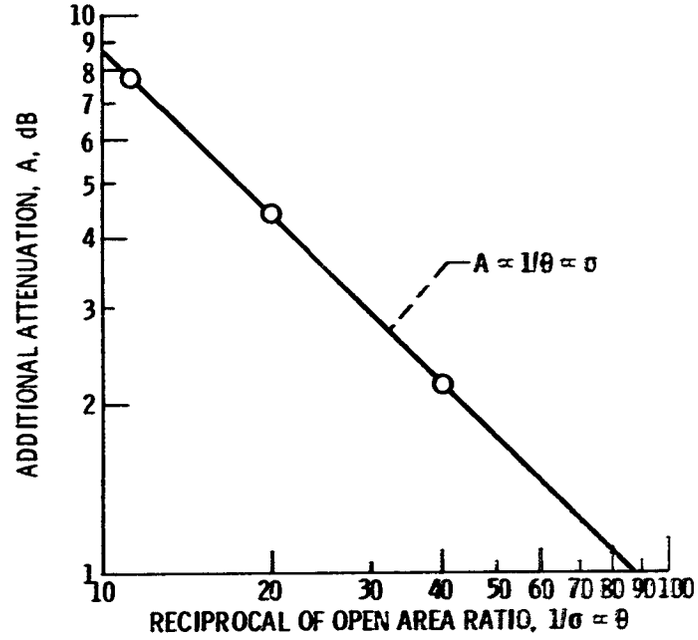


Figure 11. - Additional attenuation as a function of open area ratio and resistance, $\sigma_m$ = 7.0 percent.

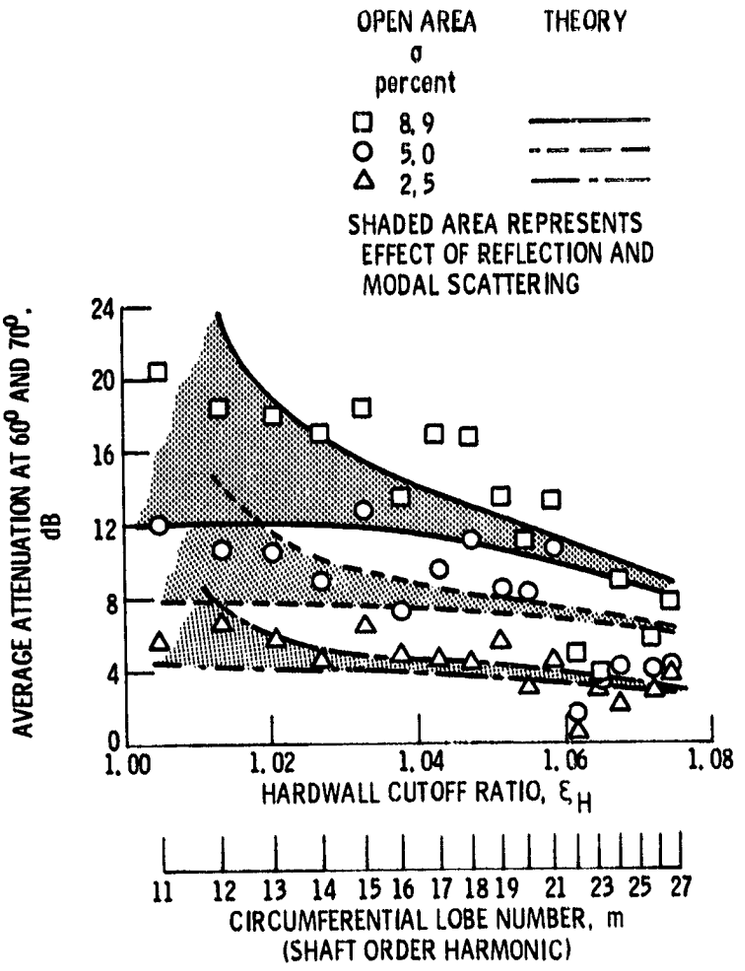


Figure 12. - MPT attenuation comparison with theory.